# Energy amplification in a parallel Blasius boundary layer flow subject to free-stream turbulence

Fu Lin and Mihailo R. Jovanović

*Abstract*—We perform an input-output analysis of transition in boundary layers subject to free-stream turbulence, which is modeled as a stochastic excitation to the Navier-Stokes equations linearized around a parallel Blasius base flow. The second order statistics of this excitation are determined by modeling energy spectrum of the homogeneous isotropic turbulence using the linearized Navier-Stokes equations. Our variance-amplification analysis identifies the near-plate streamwise streaks as the most energetic flow structures and theoretically predicts prevailing length-scales. The results of our analysis are in good agreement with the experimental and numerical studies of the free-stream-turbulence-induced boundary layer transition.

*Index Terms*—Boundary layers; energy amplification; free-stream turbulence; Navier-Stokes equations.

## I. INTRODUCTION

Boundary layers subjected to free-stream turbulence (FST) have been a topic of several recent experimental [1]–[3] and numerical [4], [5] studies. Despite simple geometry, the mechanism of transition to turbulence in boundary layers is not yet fully understood. The energy growth of background disturbance in these flows is considered as an important phase in the transition process [6]. The study of evolution of kinetic energy of perturbations reveals that nonlinear mechanism redistributes energy among different wavenumbers but has no effect on net change of energy [7]. On the other hand, linear mechanism is responsible for the growth of disturbance energy [5].

In this paper, we study the energy amplification of the linearized Navier-Stokes equations (LNSE) around parallel Blasius boundary layer (BBL) profile subject to free-stream turbulence (FST). We determine a class of spatio-temporal stochastic inputs to the linearized model capable of producing second order statistics of homogeneous isotropic turbulence (HIT). More precisely, we determine the second order statistics of forcing to the LNSE that yields energy spectrum of HIT and then study the energy amplification when forcing is introduced at different wall-normal locations of the parallel BBL flow. From our computations of the energy amplification, it is observed that the near-wall excitations are more amplified than the free-stream excitations. Our variance-amplification analysis identifies the near-wall streamwise streaks as the most energetic flow structures and theoretically predicts prevailing length-scales. The results of

our analysis are in good agreement with the experimental and numerical studies of the free-stream-turbulence-induced boundary layer transition.

The paper is organized as follows: in Section II, we describe the geometry configuration for the BBL problem. In Section III-A, we briefly summarize the energy spectrum of homogeneous isotropic turbulence. In Section III, we determine second order statistics of stochastic forcing by modeling energy spectrum of HIT using the LNSE. We present the state-space representation of the LNSE in Section IV, and describe our computational results in Section IV-B. The paper is concluded in Section V.

## II. PROBLEM SETUP

We consider the incompressible linearized Navier-Stokes equations in a Blasius boundary layer flow. The geometry configuration is shown in Fig. 1. An infinite flat plate is subject to a uniform streamwise flow $U_\infty$. The base velocity varies from zero value at the plate to the value $U_\infty$ in the free-stream. This nominal profile is homogeneous in the spanwise ($z$-direction), but spatially varying in the streamwise ($x$) and the wall-normal ($y$) directions [8]. We evaluate this nominal flow at one value of $x$ and retain its dependence of the wall-normal coordinate (in other words, we assume the nominal flow to be parallel). This parallel flow assumption is supported by [9], [10], among others. These studies show that the transient growth exhibits similar trends for the parallel and non-parallel boundary layer flows. The purpose of this study is to investigate the energy amplification by introducing certain stochastic inputs into different wall-normal locations of BBL profile. The class of stochastic inputs of interest is the one that generates HIT in a uniform stream.
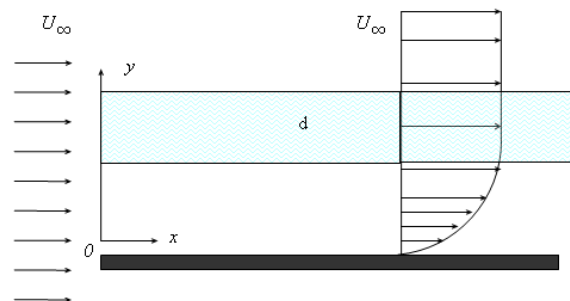


Fig. 1. Geometry configuration of BBL problem.

## III. Input Covariance using Linear System Theory

In this section, we first briefly describe the general form of energy spectrum in incompressible HIT. For rigorous mathematical derivation and additional detail we refer the reader to [11], [12]. We also determine the state-space representation of the LNSE around uniform nominal profile. This representation is used to determine input covariance that reproduces second order statistics of HIT.

### A. Energy spectrum of HIT

The initial point of this work can be concisely stated in the following question.

- What is the *second order* statistics of input forcing to the linearized Navier-Stokes equations that generates homogeneous isotropic turbulence?

The covariance of two velocity components is defined by

$$R_{ij}(r) := \mathcal{E}(u_i(r,t)u_j(x+r,t)), \quad i,j = 1,2,3$$

where $\mathcal{E}(\cdot)$ is the expectation operator, indices $i, j$ denote the corresponding components of the velocity vector $\mathbf{u} := [u_1 \ u_2 \ u_3]^T$, and $x$, $r$ are position vectors. Due to homogeneity, $R_{ij}$ is only a function of difference $r$ between two points. Moreover, under isotropic assumption $R_{ij}(r)$ becomes invariant under arbitrary rigid rotations and reflections and its Fourier transform $\Phi_{ij} := \mathcal{F}(R_{ij})$ has the following form [11]

$$\Phi_{ij}(\boldsymbol{\kappa}) = E_1(\kappa)\delta_{ij} + E_2(\kappa)k_ik_j, \quad i,j = 1,2,3.$$

Here, $k_1$, $k_2$, and $k_3$, respectively, denote the streamwise, wall-normal and spanwise wavenumbers, $\boldsymbol{\kappa} := [k_1 \ k_2 \ k_3]^T$, $\kappa^2 := k_1^2 + k_2^2 + k_3^2$, and $\delta_{ij}$ is the Kronecker delta. In incompressible flows, one can further simplify the above expression and arrive at [11]

$$\Phi_{ij}(\boldsymbol{\kappa}) = \frac{E(\kappa)}{4\pi\kappa^2}(\delta_{ij} - \frac{k_ik_j}{\kappa^2})$$

where $E(\kappa)$ is a scalar function that determines the von Karman spectrum [12]

$$E(\kappa) = LC_{vk}\frac{(\kappa L)^4}{(1 + \kappa^2 L^2)^{(17/6)}}.$$

Here, $C_{vk}$ is the normalization constant given by

$$C_{vk} = \frac{\Gamma(17/6)}{\Gamma(5/2)\Gamma(1/3)} \approx 0.48$$

and $\Gamma(\cdot)$ is the gamma function. The integral length scale $L \approx 1.5$ is numerically computed from DNS [13]. The above given $\Phi_{ij}(\boldsymbol{\kappa})$ determines the general form of energy spectrum in incompressible homogeneous isotropic turbulence.

### B. State-space representation of LNSE around uniform nominal flow

In this section, we consider LNSE and utilize spatial Fourier transform to obtain a state-space representation parameterized by wavenumbers. To address the question raised in Section III-A, we consider LNSE around uniform nominal velocity $\bar{\mathbf{u}}$,

$$\partial_t\mathbf{u} = -\nabla_{\bar{\mathbf{u}}}\mathbf{u} - \nabla_{\mathbf{u}}\bar{\mathbf{u}} - \nabla p + \frac{1}{R}\Delta\mathbf{u} + \mathbf{d}, \quad (1)$$

$$0 = \nabla \cdot \mathbf{u}, \quad (2)$$

where $\mathbf{u}$ is the fluctuation velocity, $p$ is pressure fluctuation, $R$ is the Reynolds number, $\nabla$ is the gradient, $\Delta$ is the Laplacian, and the operator $\nabla_{\mathbf{u}}$ is defined as $\nabla_{\mathbf{u}} := \mathbf{u} \cdot \nabla$.

We follow the standard conversion to obtain the evolution form of (1,2). This conversion yields the state variable $\boldsymbol{\psi} := [u_2 \ \eta]^T$, determined by the wall-normal velocity $u_2$ and vorticity $\eta := \partial_z u_1 - \partial_x u_3$. The uniform nominal flow $\bar{\mathbf{u}} := [U \ 0 \ 0]^T$ is constant in both space and time. This fact brings spatial differential operators to algebraic multiplication operators by application of Fourier transform in all spatial directions. Hence, the state-space representation of the parameterized system is given by

$$\begin{aligned} \partial_t\boldsymbol{\psi}(\boldsymbol{\kappa},t) &= A_H(\boldsymbol{\kappa})\boldsymbol{\psi}(\boldsymbol{\kappa},t) + B(\boldsymbol{\kappa})\mathbf{d}(\boldsymbol{\kappa},t), \\ \mathbf{u}(\boldsymbol{\kappa},t) &= C(\boldsymbol{\kappa})\boldsymbol{\psi}(\boldsymbol{\kappa},t). \end{aligned} \quad (3)$$

Here, $A_H$, $B$ and $C$ are given by

$$A_H := -(k^2/R + jk_1U)I_{2\times2},$$

$$B := \begin{bmatrix} -1/\kappa^2 & 0 \\ 0 & 1 \end{bmatrix} \begin{bmatrix} k_1k_2 & -k^2 & k_2k_3 \\ jk_3 & 0 & -jk_1 \end{bmatrix},$$

$$C := 1/k^2 \begin{bmatrix} -k_1k_2 & -jk_3 \\ k^2 & 0 \\ -k_2k_3 & jk_1 \end{bmatrix}, \quad k^2 := k_1^2 + k_3^2,$$

$I_{2\times2}$ denotes the identity matrix of dimension two, and each component of the stochastic input $\mathbf{d} := [d_1 \ d_2 \ d_3]^T$ is a random process in time.

### C. Determination of input covariance

The steady state covariance of the output and the state variables are defined as

$$\begin{aligned} V(\boldsymbol{\kappa}) &:= \lim_{t\to\infty}\mathcal{E}(\mathbf{u}(\boldsymbol{\kappa},t)\mathbf{u}^*(\boldsymbol{\kappa},t)), \\ \Sigma(\boldsymbol{\kappa}) &:= \lim_{t\to\infty}\mathcal{E}(\boldsymbol{\psi}(\boldsymbol{\kappa},t)\boldsymbol{\psi}^*(\boldsymbol{\kappa},t)), \end{aligned}$$

respectively, where $(\cdot)^*$ denotes the complex conjugate transpose. From state-space representation (3), these two quantities are related by

$$V(\boldsymbol{\kappa}) = C\Sigma(\boldsymbol{\kappa})C^+,$$

where $C^+$ denotes the adjoint of $C$. Using the fact that $C^+C = I$, the state covariance of homogeneous isotropic turbulence is determined by

$$\Sigma(\boldsymbol{\kappa}) = C^+\Phi(\boldsymbol{\kappa})C.$$

With some algebra, one can readily obtain the following expression

$$\Sigma(\boldsymbol{\kappa}) = \frac{E(\kappa)}{4\pi\kappa^2}I_{2\times2}.$$

The key quantity of interest is the covariance of input forcing; for temporally stationary white process $\mathbf{d}$ we have

$$\Pi(\boldsymbol{\kappa})\delta(t_1 - t_2) = \mathcal{E}(\mathbf{d}(\boldsymbol{\kappa}, t_1)\mathbf{d}^*(\boldsymbol{\kappa}, t_2)),$$

where $\Pi(\boldsymbol{\kappa})$ is a Hermitian matrix of dimension three for any triple of wavenumbers. The state covariance at steady state $\Sigma(\boldsymbol{\kappa})$ and the covariance of inputs $\Pi(\boldsymbol{\kappa})$ satisfy the Lyapunov equation [14],

$$A_H(\boldsymbol{\kappa})\Sigma(\boldsymbol{\kappa}) + \Sigma(\boldsymbol{\kappa})A_H^+(\boldsymbol{\kappa}) = -B(\boldsymbol{\kappa})\Pi(\boldsymbol{\kappa})B^+(\boldsymbol{\kappa}). \quad (4)$$

Our objective is to determine $\Pi(\boldsymbol{\kappa})$ that gives the covariance matrix of HIT. It is easy to show that

$$\frac{E(\kappa)}{4\pi\kappa^2}I_{2\times 2} = B(\boldsymbol{\kappa})\Pi(\boldsymbol{\kappa})B^+(\boldsymbol{\kappa}). \quad (5)$$

To solve (5) for $\Pi(\boldsymbol{\kappa})$, one may observe that there is a discrepancy between the number of variables and the number of equations. On the one hand, there are six unknowns in the 3-by-3 Hermitian matrix $\Pi(\boldsymbol{\kappa})$; on the other hand, there are only three equations due to the fact that left hand side of (4) has dimension of two. This implies that the solution for $\Pi(\boldsymbol{\kappa})$ is not unique. Equivalently, the input matrix $B(\boldsymbol{\kappa})$ is not left invertible. However, the underlying reason for the loss of uniqueness can be traced back to the LNSE (1,2) where we eliminated one velocity variable due to continuity constraint. To obtain uniqueness, one may accordingly devise an appropriate constraint between input variables. In this paper, we will consider solenoidal, i.e., divergence-free inputs

$$\nabla \cdot \mathbf{d} = 0.$$

In a similar fashion for state variables, the inputs are organized as $d_s := [d_2 \ d_\eta]$ which transforms the $B$-matrix to $B_s := I_{2\times 2}$.

The main reason for this choice of constraint stems from the direct numerical simulations showing that solenoidal inputs with bounded spectrum is capable of generating isotropic turbulence [15]. Moreover, both operator $B$ and its adjoint $B^+$ then simplify to identity operator. Hence, the covariance of solenoidal inputs is determined by

$$\Pi_s(\kappa) = \frac{E(\kappa)}{4\pi\kappa^2}I_{2\times 2}.$$

This covariance is used in the next section to model a stochastic excitation to the Navier-Stokes equations linearized around a parallel Blasius base flow.

### IV. STOCHASTICALLY FORCED BLASIUS BOUNDARY LAYER

In this section, we determine the state-space representation of the Navier-Stokes equations linearized around BBL profile and compute the energy amplification [16], [**?**] for the input forcing with covariance determined in Section III.

#### A. State-space representation of LNSE around BBL profile

As described in section II, the BBL nominal flow profile is homogeneous in spanwise direction but not in streamwise and wall-normal directions. Under the assumption of parallel base flow, we can apply spatial Fourier transform in both streamwise and spanwise directions. Hence, the state-space representation of LNSE around BBL nominal profile $U_B(y)$ is given by

$$\partial_t \boldsymbol{\psi}(k_1, y, k_3, t) = [A_B(k_1, k_3)\boldsymbol{\psi}(k_1, k_3, t)](y) +$$
$$[B(k_1, k_3)\mathbf{d}(k_1, k_3, t)](y)$$
$$\mathbf{u}(k_1, y, k_3, t) = [C(k_1, k_3)\boldsymbol{\psi}(k_1, k_3, t)](y).$$
$$(6)$$

The operators $A_B, B$ and $C$ are given by

$$A_B := \begin{bmatrix} A_{11} & 0 \\ A_{21} & A_{22} \end{bmatrix},$$

$$B := \begin{bmatrix} \Delta^{-1} & 0 \\ 0 & I \end{bmatrix}\begin{bmatrix} -jk_1\partial_y & -k^2 & -jk_3\partial_y \\ jk_3 & 0 & -jk_1 \end{bmatrix}$$

$$C := \begin{bmatrix} C_{u1} \\ C_{u2} \\ C_{u3} \end{bmatrix} = 1/k^2 \begin{bmatrix} jk_1\partial_y & -jk_3 \\ k^2 & 0 \\ jk_3\partial_y & jk_1 \end{bmatrix}.$$

Here

$$A_{11} := -jk_1\Delta^{-1}U_B\Delta + jk_1\Delta^{-1}U_B'' + \tfrac{1}{R}\Delta^{-1}\Delta^2,$$

$$A_{21} := -jk_3U_B',$$

$$A_{22} := -jk_1U_B + \tfrac{1}{R}\Delta,$$

where $U_B' := dU_B(y)/dy$, $\Delta := \partial_{yy} - k^2$, and $\Delta^2 := \partial_{yyyy} - 2k^2\partial_{yy} + k^4$. The boundary conditions are given by

$$v(k_1, 0, k_3, t) = \partial_y v(k_1, 0, k_3, t) = 0,$$
$$v(k_1, \infty, k_3, t) = \partial_y v(k_1, \infty, k_3, t) = 0,$$
$$\eta(k_1, 0, k_3, t) = \eta(k_1, \infty, k_3, t) = 0,$$
$$\forall k_1, k_3 \in \mathbb{R}, \quad \forall t \geq 0.$$

We will consider the situation in which input forcing $\mathbf{d}(x, y, z, t)$ has an intensity that varies with the wall-normal direction. More precisely, we assume that a filtered excitation $\mathbf{d} := f(y)\mathbf{d_s}$ enters the state equation, where $f(y)$ is a smooth filter function

$$f(y) := \frac{1}{\pi}(\text{atan}(y - y_1) - \text{atan}(y - y_2)).$$

The parameters $y_1$ and $y_2$ can be chosen to determine the shape of filter $f(y)$. For example, for $y_1 = 5, y_2 = 10$, $f(y)$ is plotted in Fig. 2. It is convenient to incorporate the function $f(y)$ into operator $B$ by defining

$$\begin{aligned} B_B &:= Bf(y) \\ &= \begin{bmatrix} \Delta^{-1}(f(y)\Delta + f'(y)\partial_y) & 0 \\ 0 & f(y) \end{bmatrix} \end{aligned}$$

Then, (6) can be rewritten as

$$\partial_t \boldsymbol{\psi}(k_1, y, k_3, t) = [A_B(k_1, k_3)\boldsymbol{\psi}(k_1, k_3, t)](y) +$$
$$[B_B(k_1, k_3)\mathbf{d_s}(k_1, k_3, t)](y)$$
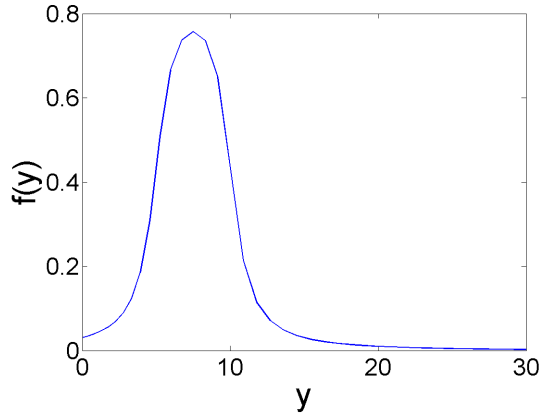$$\mathbf{u}(k_1, y, k_3, t) = [C(k_1, k_3)\boldsymbol{\psi}(k_1, k_3, t)](y).$$
$$(7)$$

Fig. 2. The shape of filter function $f(y)$ with $y_1 = 5, y_2 = 10$.

The purpose of this paper is to quantify receptivity of the LNSE subject to white (in time) solenoidal stochastic excitation with second order statistics determined in Section III.

### B. Computation of energy amplification

We compute energy amplification utilizing the standard fact that the $H_2$ norm can be calculated from the solution to the Lyapunov equation. The frequency response of system (7) is given by

$$H(k_1, k_3, \omega) = C(k_1, k_3)(j\omega I - A_B(k_1, k_3))^{-1}B_B(k_1, k_3),$$

where $\omega$ is the temporal frequency. Therefore, the input-output relationship of system (7) can be presented by

$$\mathbf{u}(k_1, y, k_3, \omega) = [H(k_1, k_3, \omega)\mathbf{d_s}(k_1, k_3, \omega)](y).$$

To study the energy amplification, we choose the $H_2$ system norm defined as

$$\|H\|_2^2(k_1, k_3) := \frac{1}{2\pi} \int_{-\infty}^{\infty} \|H(k_1, k_3, \omega)\|_{HS}^2 d\omega,$$

where $\| \cdot \|_{HS}$ is the Hilbert-Schmidt norm of an operator defined by

$$\|H\|_{HS}^2 := \text{trace}(HH^+).$$

For fixed wavenumber pair $(k_1, k_3)$ and fixed $\omega$, $H$ is an operator in $y$-direction. The $H_2$ norm quantifies the variance (energy) amplification of harmonic (in $x$ and $z$) stochastic (in $y$ and $t$) disturbances at any given wavenumber pair $(k_1, k_3)$. It is a standard fact that $H_2$ norm can be computed using solution to the operator Lyapunov equation

$$\begin{aligned} A_B(k_1, k_3)X(k_1, k_3) + X(k_1, k_3)A_B^+(k_1, k_3) \\ = -B_B(k_1, k_3)\Pi_s(k_1, k_3)B_B^+(k_1, k_3). \end{aligned} \quad (8)$$

The $H_2$ norm is then determined by

$$\|H\|_2^2(k_1, k_3) = \text{trace}(C(\boldsymbol{\kappa})X(k_1, k_3)C^+(k_1, k_3))).$$

In the sequel, we briefly describe the numerical computation of $H_2$ norm using a Chebyshev collocation scheme [17]. In the streamwise and spanwise directions, we grid over the

wavenumber space (uniformly in logarithmic scale in $k_1$ with $k_{1min} = 10^{-4}$, $k_{1max} = 10^{-1}$, and uniformly in linear scale in $k_3$ with $k_{3min} = 0.01$, $k_{3max} = 1$). In the wall-normal semi-infinite direction, we approximate the domain from plate boundary to the free-stream region with a box $y \in [0, L_y]$ of size $L_y = 25$. A Chebyshev collocation scheme [17] is employed to discretize the operators $A_B$, $B_B$ and $C$ with $N = 100$ Gauss-Lobatto points in $y$. By increasing both $L_y$ and $N$, it is confirmed that the box-size is large enough and the resolution of discretization is high enough to secure convergence of numerical approximation.

### C. Numerical computation results

We present results obtained by computing the $H_2$ norm of stochastically excited Blasius boundary layer with $R = 500$ (see Fig. 3 for nominal velocity profile). The flow structures contributing most to the energy amplification are also discussed in this section. The solenoidal excitation is
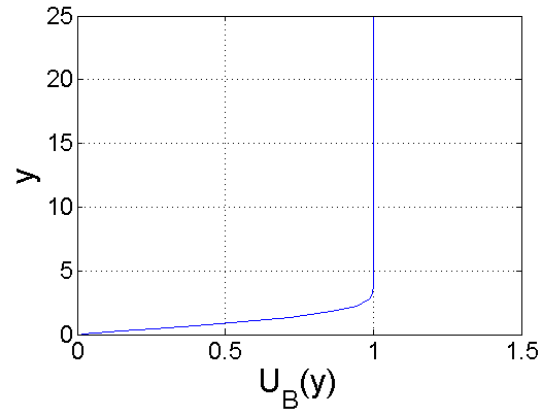


Fig. 3. Nominal BBL profile with $R = 500$.

first introduced to the free-stream region by filtering through pre-specified function $f(y)$. From Fig. 4, it is observed that energy is most amplified at low streamwise wavenumber value, $k_1 \approx 0$. However, a global peak takes place at $k_3 \approx 0.34$. Note that the results are presented in logarithmic scale of base ten.

It is of interest to investigate energy amplification with input forcing introduced to different locations in wall-normal direction. The whole box range in wall-normal direction $[0, L_y]$ is divided equally into five regions with the notation that the first region denotes $[0, L_y/5]$ and the second region denotes $[L_y/5, 2L_y/5]$, etc.. The solenoidal input forcing then excites BBL at each of the first four regions and the results are given in Fig. 5. It turns out that the energy is amplified most when flow is excited near plate boundary. The peak value at 1st region is greater than peak values in any other regions with a difference of more than half order of magnitude. Another observation is that as inputs shift from plate boundary towards free-stream turbulence region, the peak in spanwise direction shifts to lower values of $k_3$.

To obtain more detailed results at low frequency, we set $k_1 = 0$ and grid in $k_3$ and then vice versa. In both these cases,
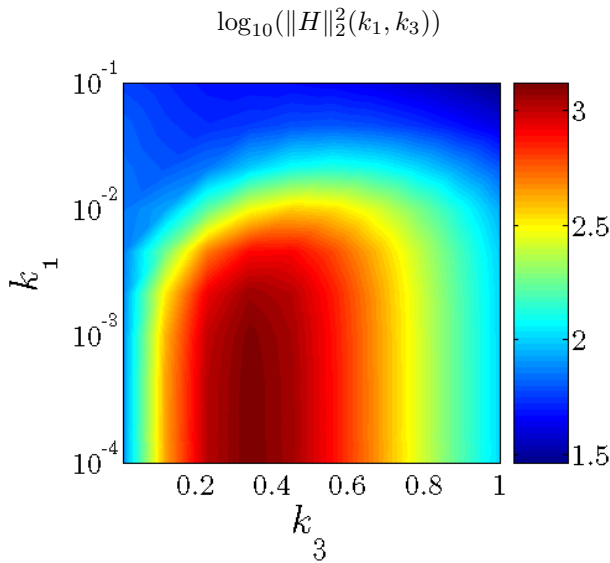
$$\log_{10}(\|H\|_2^2(k_1, k_3))$$

Fig. 4. Plot of $\log_{10}(\|H\|_2^2(k_1, k_3))$ in BBL profile subject to FST with $R = 500$.
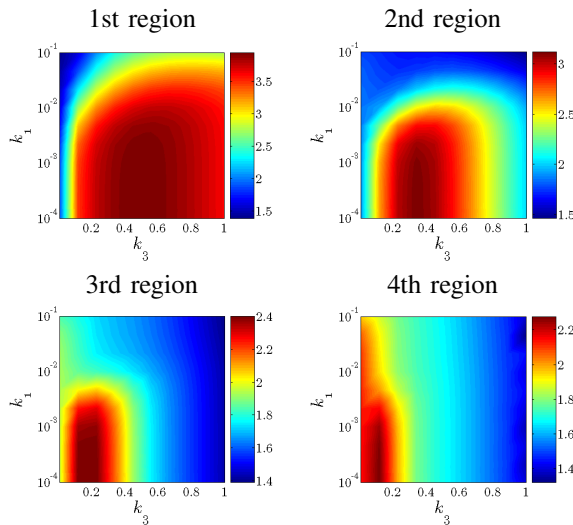


Fig. 5. Plots of $\log_{10}(\|H\|_2^2(k_1, k_3))$ in BBL flow with $R = 500$ subject to stochastic excitation at each of four different wall-normal regions.

we introduce input forcing in different regions as before. In case of streamwise constant excitation, i.e. $k_1 = 0$, the result in Fig. 6 confirms previous observations. First, near-wall excitations are amplified most and their peak values are at least one order of magnitude larger compared to the the peak values obtained by exciting in other wall-normal regions. Secondly, the peak shifts to lower values of $k_3$ as the excitation region shifts from plate boundary to the free-stream region. In case of spanwise constant excitation $k_3 = 0$, it is observed that the $H_2$ norm is much smaller than for streamwise constant perturbations. An interesting and important observation can be made from Fig. 7. For excitations entering in the 2nd, 3rd and 4th regions, the $H_2$ norm decreases monotonically as $k_1$ increases while a peak is uncovered at $k_1 \approx 0.31$ in case of the near-wall excitation.

This peak corresponds to the Tollmien-Schlichting (TS) wave, which represent the eigenfunctions corresponding to the "poorly damped" system modes (that is, the eigenvalues in the immediate vicinity of the imaginary axis).
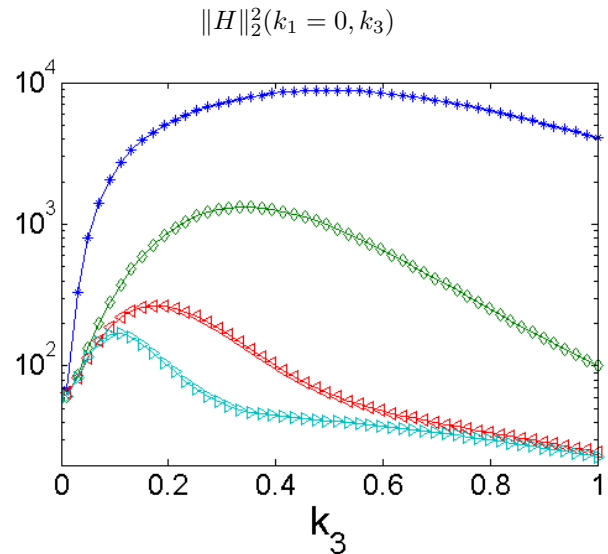


$$\|H\|_2^2(k_1 = 0, k_3)$$

Fig. 6. Plot of $\|H\|_2^2(k_1 = 0, k_3)$ in BBL flow with $R = 500$ for stochastic excitation at each of four different wall-normal regions. From the top to the bottom, the four curves correspond to 1st, 2nd, 3rd and 4th region, respectively.

The structure of eigenvector of state covariance $X$ associated with the largest eigenvalue is of interest to observe. This eigenvector determines the flow structures that produce most variance in stochastically excited BBL flow. The eigenvector $\psi$ associated with the most amplified mode is computed by eigenvalue decomposition of covariance matrix $X$. For example, $u_1 := C_{u1}\psi$ represents the structure of the corresponding streamwise velocity. The results are plotted in physical domain as given in Fig. 8. Our variance-amplification analysis show that free-stream turbulence penetrates the boundary layer and produces the near-plate streamwise streaks as the most energetic flow structures. The results of our analysis are in good agreement with the experimental and numerical studies of the free-stream-turbulence-induced boundary layer transition.

## V. CONCLUDING REMARKS

In this paper, we study the energy amplification of the linearized Navier-Stokes equations around parallel Blasius boundary layer profile subject to free stream turbulence. It is shown that the LNSE model is capable of producing second order statistics of HIT using the class of solenoidal stochastic input forcing. We used this forcing as a stochastic input to the linearized Navier-Stokes equations and illustrated that regions in which excitation enters significantly influence the values of frequency response peaks. Our variance-amplification analysis identifies the near-plate streamwise streaks as the most energetic flow structures irrespective of the region in which excitation enters. The results of
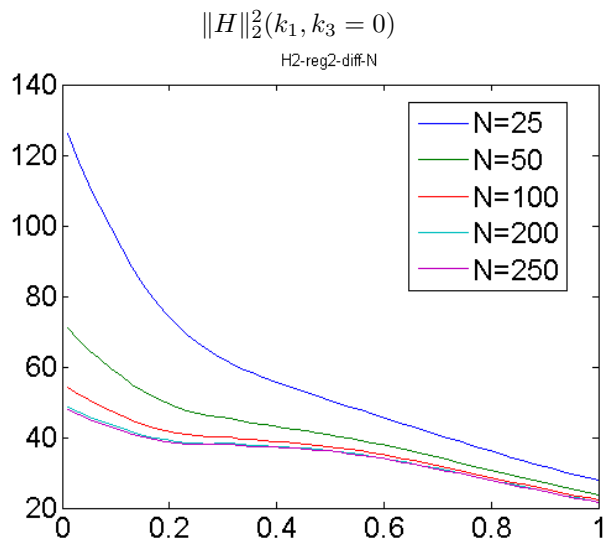
$$\|H\|_2^2(k_1, k_3 = 0)$$

Fig. 7. Plot of $\|H\|_2^2(k_1, k_3 = 0)$ in BBL flow with $R = 500$ for stochastic excitation at each of four different wall-normal regions. From the bottom to the top (cf. Fig. 6), the four curves correspond to 1st, 2nd, 4th and 3rd region, respectively.
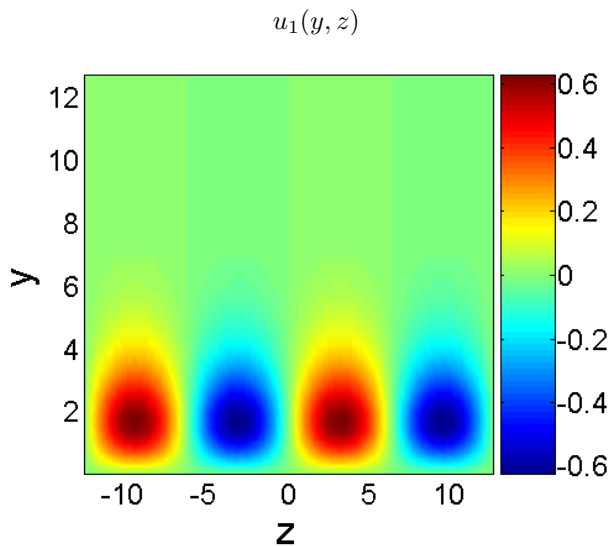


$$u_1(y, z)$$

Fig. 8. Flow structures that produce most variance in parallel BBL flow with $R = 500$.

our analysis are in good agreement with the experimental and numerical studies of the free-stream-turbulence-induced boundary layer transition.

## REFERENCES

[1] M. Matsubara and P. H. Alfredsson, "Disturbance growth in boundary layers subjected to free-stream turbulence," *Journal of fluid mechanics*, vol. 430, 2001.

[2] J. M. Kendall, "Experiments on boundary-layer receptivity to freestream turbulence," *AIAA*, 1998.

[3] K. J. A. Westin, "Laminar turbulent boundary layer transition influenced by free stream turbulence," Ph.D. dissertation, Department of Mechanics, KTH, 1997.

[4] R. G. Jacobs and P. A. Durbin, "Simulations of bypass transition," *J. Fluid Mech.*, vol. 428, pp. 185–212, 2001.

[5] L. Brandt, P. Schlatter, and D. S. Henningson, "Transition in boundary layers subject to free-stream turbulence."

[6] K. M. Butler and B. F. Farrell, "Three-dimensional optimal perturbations in viscous shear flow," *Phys. Fluids A*, vol. 4, p. 1637, 1992.

[7] P. J. Schmid and D. S. Henningson, *Stability and Transition in Shear Flows*. New York: Springer-Verlag, 2001.

[8] R. L. Panton, *Incompressible flows*. New York: John Wiley & Sons, Inc., 1996.

[9] S. Berlin and D. S. Henningson, "A nonlinear mechanism for receptivity of free-dtream diturbances," *Phys. Fluids*, vol. 11, pp. 3749–3760, 1999.

[10] A. Tumin and E. Reshokto, "Spatial theory of optimal disturbances in boundary layers," *Phys. Fluids*, vol. 13, pp. 2097–2104, 2001.

[11] G. K. Batchelor, *The Theory of Homogeneous Turbulence*. Athenaeum Press, 1953.

[12] P. A. Durbin and B. A. P. Reif, *Theory and modeling of turbulent flows*. Wiley, 2000.

[13] L. Wang, S. Chen, J. G. Brasseur, and J. C. Wyngaard, "Examination of hypotheses in the kolmogorov refined turbulence theory through high-resolution simulations. part 1. velocity field," *J. Fluid Mech*, vol. 309, pp. 113–156, 1996.

[14] K. Zhou, J. C. Doyle, and K. Glover, *Robust and optimal control*. Upper Saddle River, NJ, USA: Prentice-Hall, Inc., 1996.

[15] T. Gotoh, D. Fukayama, and T. Nakano, "Velocity field statistics in homogeneous steady turbulence obtained using a high-resolution direct numerical simulation," *Physics of Fluids*, vol. 14, pp. 1065–1081, Mar. 2002.

[16] B. Bamieh and M. Dahleh, "Energy amplification in channel flows with stochastic excitation," *Phys. Fluids*, vol. 13, no. 11, pp. 3258–3269, 2001.

[17] J. Weideman and S. Reddy, "A matlab differentiation matrix suite," *ACM Trans. on Mathematical Software*, vol. 26, no. 4, pp. 465–519, 2000.